13th Scientific/Research Symposium with International Participation
„METALLIC AND NONMETALLIC MATERIALS“, B&H, 27th May 2021

INFLUENCE OF MICROALLOYING WITH BORON, ZIRCONIUM AND TELLURIUM ON THE MODIFICATION OF NONMETALLIC INCLUSIONS OF AUSTENITIC STAINLESS STEEL WITH SULPHUR ADDITION

Derviš Mujagić[1], Aida Imamović[2], Mustafa Hadžalić[1]
[1] University of Zenica, Institute ″Kemal Kapetanović″
Zenica
Bosnia and Herzegovina

[2] University of Zenica, Faculty of Metallurgy and Technology
Zenica
Bosnia and Herzegovina

Keywords: microstructure, nonmetallic inclusions, sulphur, boron, zirconium, tellurium

ABSTRACT
The basic characteristics of the chemical composition of steel with improved machinability (X8CrNiS18-9) are the increased content of sulphur (0.15-0.45%), phosphorus (0.07-0.11%) and manganese (0.5-1.5%).
Sulphur by creating sulphide inclusions reduces friction and cutting resistance, and increases the brittleness of the chip.Considering its harmful effect in steel, as well as the fact that non-metallic inclusions have been insufficiently tested for this type of high-alloyed steel, the aim of this research is to determine by microalloying the possibility of modification of non-metallic inclusions. Modification with boron and zirconium favorably affects the ductile properties of steel, and a step forward in this study is a modification of inclusions with tellurium.
It is of particular importance to determine the behavior of non-metallic inclusions in the process of production of the structural part and in subsequent exploitation. Therefore, plastic processing of austenitic stainless steel was also carried out, forging and rolling with two different level of processing.

1. INTRODUCTION
Stainless steel is an ideal material to create lasting solutions in demanding applications. Its uses are endless. Thanks to its unique properties such as durability, low-maintenance and resistance to corrosion, stainless steel is not only the strongest, but also the most economically sustainable choice. [1].
Since 1950, stainless steels have seen the greatest increase in consumption, with the most frequent, austenitic [2].
In addition to alloying with at least 10.5% chromium, for stainless steel to be corrosion-resistant (passive), another condition must be fulfilled, namely the existence of a homogeneous single-phase ferrite, austenitic or martensitic microstructure [3].

The use of stainless steels is small compared to carbon steels, but shows steady growth, Figure 1. [4]. In Figure 2. [4], which shows the annual growth rate of major metals from 1980 to 2018, it is easy to see that the growth rate of stainless steels is by far the highest.

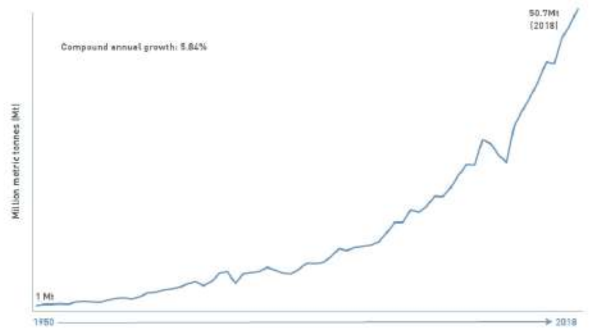

Figure 1. Compound annual growth rate of world stainless melt shop production 1950-2018 [4]

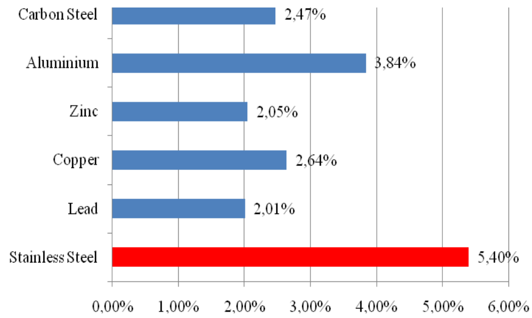

Figure 2. Compound annual growth rate of major metals (% / year): 1980 - 2018 [4]

Stainless steel is the most recycled material in the world and it is estimated that 82% of stainless steel used is recycled into new steel. When recycled, melted recycled steel has as good qualities and properties as the original steel. Today, approximately 60% of the raw materials used for the production stainless steels are recycled steels [5].

2. INFLUENCE OF ALLOYING ELEMENTS IN STEEL

Manganese is most commonly used as a deoxidizer and desulphuriser during steel production. Due to its high affinity for sulphur, manganese produces MnS sulphide, thus preventing the negative effect of FeS sulphide [3].
High sulphur content has a positive effect on machinability characteristics. Tool wear is reduced, and chip separation is more favorable [6].
Boron in the stainless austenitic steels allows precipitation hardening (increase in yield strength and tensile strength), but lowers resistance to general corrosion [3].
Zirconium addition causes sulphide inclusions to be spherical (globular) rather than elongated, which improves the strength and ductility of microalloyed cast steel [7].
The presence of *tellurium* in steel leads to the formation of globular sulphide inclusions, which at the same time favorably affect the machinability of steel, since its presence in steel reduces the energy required to separate the material in the shear zone during cutting [8].
Tellurium forms manganese telluride (MnTe) inclusions and is apparently more effective than the sulphur for machinability of austenitic stainless steels. It also *promotes globularization and expansion of sulphide inclusions* [9].

3. NONMETALLIC INCLUSIONS

Nonmetallic inclusions form separate phases. Nonmetallic phases containing more than one compound (eg different oxides, oxide + sulphide) are called complex nonmetallic inclusions (spinels, silicates, oxisulphides, carbonitrides) [10].
In order to produce steels with the best machinability, a number of inclusions with a carefully designed composition are required [11].
Manganese sulphide inclusions tend to elongate in the rolling direction, and elongated manganese sulphide inclusions are less desirable from a machinability standpoint than globular manganese sulphide inclusions. Also, from a machinability standpoint, smaller manganese sulphide inclusions are considered less desirable than larger inclusions [12].

Non-metallic inclusions adversely affect many properties sensitive to the continuity of the steel structure, while they have little or no effect on other properties [13].
The presence of inclusions also affects the machinability of the steel, the hard oxides exacerbate, and the soft manganosulfides improve the machinability [14].

4. EXPERIMENTAL RESEARCH AND TEST RESULTS

The melting and casting of austenitic stainless steel X8CrNiS18-9 was carried out in a vacuum induction furnace with a capacity of 20 kg, with a maximum power of 40 kW, and is located at the Department for melting and metal casting of the Institute "Kemal Kapetanović".
Eight meltings were done. The first melt is austenitic stainless steel X8CrNiS18-9 without alloying elements. Subsequently, in the following seven melt, the composition with the corresponding contents of boron, zirconium and tellurium was modified so that each of the above elements was added independently, then in combinations with two, and finally with all three alloying elements. Chemical analyzes of all melt variants are given in Table 1 [15].

Table 1. Chemical analyzes of all melt variants [15]

Melt variants	*Chemical composition (%)*									
	C	*Si*	*Mn*	*P*	*S*	*Cr*	*Ni*	*B*	*Zr*	*Te*
without alloying elements	0,03	0,42	0,61	0,021	0,18	18,3	9,4	–	–	–
alloyed with B	0,05	0,47	0,66	0,021	0,19	18,5	9,5	0,004	–	–
alloyed with Zr	0,04	0,35	0,75	0,021	0,17	18,8	9,4	–	0,016	–
alloyed with Te	0,05	0,40	0,80	0,010	0,16	18,9	9,3	–	–	0,033
alloyed with B i Zr	0,04	0,49	0,69	0,012	0,17	18,5	9,1	0,004	0,009	–
alloyed with B i Te	0,04	0,35	0,78	0,011	0,18	18,8	9,3	0,004	–	0,039
alloyed with Zr i Te	0,03	0,47	0,72	0,012	0,18	18,5	8,9	–	0,007	0,040
alloyed with B, Zr i Te	0,04	0,44	0,78	0,012	0,19	17,1	9,3	0,006	0,012	0,042

4.1. Metallographic testing of casted samples

All ingots are subjected to heat treatment: solution annealing – heating to 1050 °C, followed by rapid cooling in water. After the heat treatment, samples were taken next to the ingot head for metallographic testing of the cast state (Figure 3 - after grinding and polishing).
Subsequently, an analysis of the content, size and distribution of the nonmetallic inclusions in the unetched state was performed, and the results of the tests are given in Table 2. The imaging of samples under a specific magnification (x50) was performed on an Olympus PMG3 type optical microscope, and one image was given for each sample (Figure 4). The figures show inclusions of average size, while Table 2 also lists individual inclusions that are significantly larger than average.


Figure 3. Casted samples for metallographic tests [15]

Table 2. Results of metallographic testing of casted samples [15]

Melt variants	*Size of sulphide inclusions (μm)*		*The total number of inclusions by zones **			*Note*
			I	*II*	*III*	
without alloying elements	200,1 150,0 90,0 85,0	60,1 55,5 40,8	7	8	4	Lots of small sulphide inclusions; Size porosities 264 i 140μm
alloyed with B	221,2 125,7	92,8 37,1	7	5	6	Lots of small sulphide inclusions
alloyed with Zr	115,3 193,1	69,2	3	3	6	Lots of small sulphide inclusions
alloyed with Te	162,1 110,8	63,1	1	5	7	Lots of small sulphide inclusions
alloyed with B i Zr	64,0 100,8	150,0 104,0	8	2	8	Lots of small sulphide inclusions
alloyed with B i Te	31,0 25,0	120,0 28,0	3	1	2	Lots of small sulphide inclusions
alloyed with Zr i Te	54,0 75,0 102,0	168,0 184,0	4	8	8	Lots of small sulphide inclusions
alloyed with B, Zr i Te	110,0 90,0	80,0 35,0	4	Small inclusions	Small inclusions	Lots of small sulphide inclusions; Porosity observed

* Zones I, II and III represent sample areas, so that zones I and III represent the edges of the sample, while zone II represents the central part of the sample.

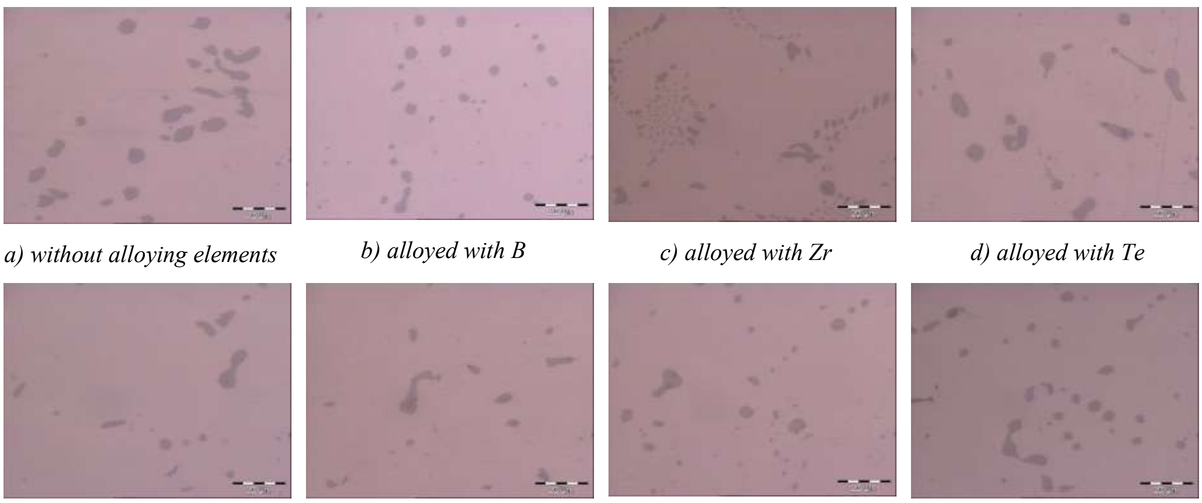

a) without alloying elements *b) alloyed with B* *c) alloyed with Zr* *d) alloyed with Te*

e) alloyed with B i Zr *f) alloyed with B i Te* *g) alloyed with Zr i Te* *h) alloyed with B, Zr i Te*

Figure 4. Microstructure of all melt variants for the casted state [15]

4.2. Metallographic testing of forged samples

After solution annealing, the specimens were hot deformed, namely forging on a hydraulic press with a power of 44 kW and a hammer with a power of 24 kW, which are located at the Department for Plastic Processing of Metals of the Kemal Institute "Kemal Kapetanović", up to a dimension of ϕ 50 mm.

The samples, after the completion of forging process and rough machining, are shown in Figure 5. Upon completion of the forging process, samples were taken to perform metallographic testing for the forging condition (Figure 6).

Figure 5. The samples after the completion of forging process and rough machining [15]

Figure 6. Forged samples for metallographic tests [15]

As with the cast samples, an analysis of the content, size and distribution of the nonmetallic inclusions in the unetched state was performed, and the test results are given in Table 3. Samples were also imaging on an OLYMPUS PMG3 type optical microscope (x50), and one image was taken for each sample (Figure 7).

Table 3. Results of metallographic testing of forged samples [15]

<table>
<tr><th>Melt variants</th><th colspan="3">Size of inclusions (μm)</th><th>Note</th></tr>
<tr><td rowspan="2">without alloying elements</td><td colspan="3">Complex globular inclusions:</td><td rowspan="2">Lots of small sulphide inclusions</td></tr>
<tr><td>50,0</td><td colspan="2">90,0</td></tr>
<tr><td>alloyed with B</td><td colspan="3">The longest sulphide inclusion:
~ 80,0</td><td>Lots of small sulphide inclusions</td></tr>
<tr><td rowspan="2">alloyed with Zr</td><td colspan="3">Complex inclusions:</td><td rowspan="2">Lots of small sulphide inclusions</td></tr>
<tr><td>50,0 x 20,0</td><td>25,0 x 20,0</td><td>48,0 x 18,0</td></tr>
<tr><td>alloyed with Te</td><td colspan="3">Globular inclusion: ~ 20,0
Complex inclusion: 139,0 x 30,0</td><td>Lots of small sulphide inclusions</td></tr>
<tr><td>alloyed with B i Zr</td><td colspan="3">Complex inclusion: 50,0 x 10,0</td><td>Lots of small sulphide inclusions</td></tr>
<tr><td rowspan="2">alloyed with B i Te</td><td colspan="3">Complex inclusions:</td><td rowspan="2">Lots of small sulphide inclusions;
One nest of complex inclusions</td></tr>
<tr><td>63,0 x 18,0</td><td colspan="2">126,0 x 10,0</td></tr>
<tr><td rowspan="2">alloyed with Zr i Te</td><td colspan="3">Complex inclusions:</td><td rowspan="2">Lots of small sulphide inclusions</td></tr>
<tr><td>70,0 x 30,0</td><td colspan="2">150,0 x 30,0</td></tr>
<tr><td rowspan="2">alloyed with B, Zr i Te</td><td colspan="3">Complex inclusions:</td><td rowspan="2">Lots of small sulphide inclusions</td></tr>
<tr><td>350,0 x 80,0</td><td colspan="2">50,0 x 20,0</td></tr>
</table>

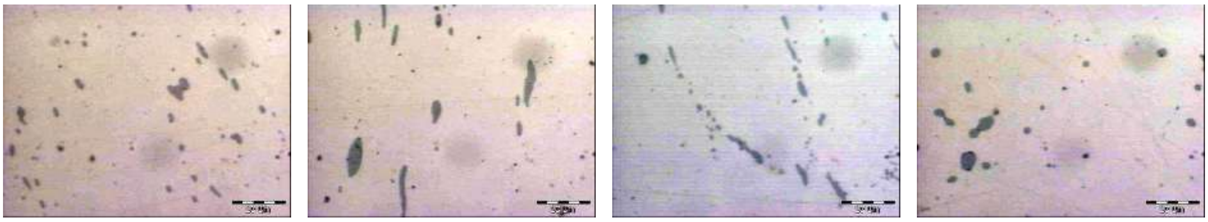

a) without alloying elements *b) alloyed with B* *c) alloyed with Zr* *d) alloyed with Te*

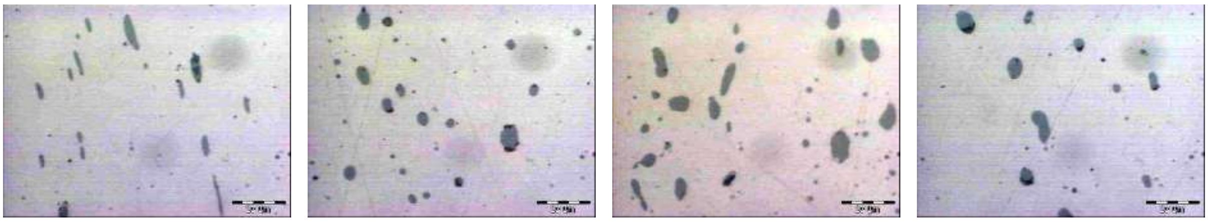

e) alloyed with B i Zr *f) alloyed with B i Te* *g) alloyed with Zr i Te* *h) alloyed with B, Zr i Te*

Figure 7. Microstructure of all melt variants for forged state [15]

4.3. Metallographic testing of rolled samples

The rolling was performed on the SKET rolling mill, with the first section being reduced to 18 mm, while the second one reached a final sample size of 14 x 50 mm. The rolling speed was 400 rpm. After completion of rolling, all samples were quenched in water in order to avoid the effect of sensitisation. All samples are of different lengths depending on the amount of material in each variant. Figure 8 shows all the samples after the rolling process has been carried out. Upon completion of the second stage of deformation (rolling to dimensions 14 x 50 mm), samples were taken to perform metallographic testing for the rolling condition (Figure 9).

Figure 8. The samples after the rolling process was performed [15]

Figure 9. Rolled samples for metallographic tests [15]

As with the previous samples, the content, size and distribution of nonmetallic inclusions in the unetched state were analyzed, and the test results are given in Table 4. The test for the rolling condition was performed in accordance with ASTM E45-11 – Standard Test Methods for Determining the Contents of Inclusions in Steel. BAS EN 10088-1 does not specify limit values for the content of nonmetallic inclusions. Sample imaging under a certain magnification (x50) was performed on an OLYMPUS PMG3 type optical microscope, and one image was given for each sample (Figure 10).

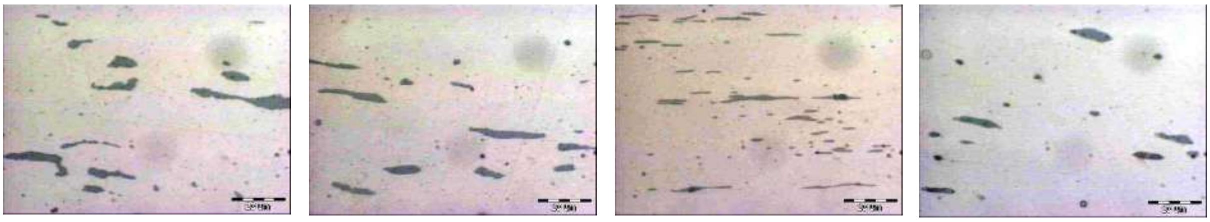

a) without alloying elements *b) alloyed with B* *c) alloyed with Zr* *d) alloyed with Te*

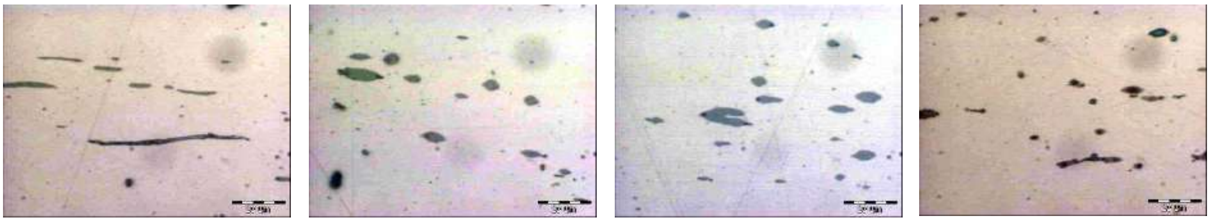

e) alloyed with B i Zr *f) alloyed with B i Te* *g) alloyed with Zr i Te* *h) alloyed with B, Zr i Te*

Figure 10. Microstructure of all melt variants for rolled state [15].

Table 4. Results of metallographic testing of rolled samples [15]

Melt variants	*Sulphides*		*Note*
	Thin	*Thick*	
without alloying elements	3	1,5	Many small sulphide inclusions with thickness less than 2μm have been observed. A complex inclusion of 250 *μm* size was also observed.
alloyed with B	3	1	Many small sulphide inclusions with thickness less than 2μm have been observed.
alloyed with Zr	3	3	Many small sulphide inclusions with thickness less than 2μm have been observed. A complex oxysulfide inclusion of 500 μm size was also observed.
alloyed with Te	3	3	Many small sulphide inclusions with thickness less than 2μm have been observed. Complex inclusions of size 600, 500, 300, 200 μm were also observed.
alloyed with B i Zr	1,5	3	Many small sulphide inclusions with thickness less than 2μm have been observed. Complex inclusions of size 600, 300 μm were also observed.
alloyed with B i Te	1,5	1	Many small sulphide inclusions with thickness less than 2μm have been observed. A complex inclusion of 150 μm size was also observed.
alloyed with Zr i Te	1,5	3	Many small sulphide inclusions with thickness less than 2μm have been observed. Complex inclusions of size 600, 150, 60 μm were also observed.
alloyed with B, Zr i Te	1,5	3	Many small sulphide inclusions with thickness less than 2μm have been observed. Complex inclusions of size 500 μm were also observed.

5. CONCLUSIONS

Based on experimental research, it is possible to make the following conclusions:

- In experimental melts after rolling and after heat treatment, the presence of type A inclusions (sulphides) according to ASTM E45-11 was detected. The largest number of inclusions and the biggest inclusions were determined for tellurium alloyed melt, and for variants of melts alloyed with boron and zirconium and zirconium and tellurium elements.
- The influence on the shape and size of the nonmetallic inclusions is especially shown by zirconium and tellurium;
- Addition of tellurium with zirconium and boron improves the globularization of austenitic stainless steel X8CrNiS18-9, in this respect tellurium is particularly dominant;
- Elements of boron, zirconium and tellurium are added for the purpose of modifying sulfide inclusions, in particular their globularization and thickness increase. This work confirmed this, especially in the case of zirconium and tellurium.

6. REFERENCES:

[1] http://www.outokumpu.com/sitecollectiondocuments/outokumpu-stainless-steel-handbook.pdf (december 2019)

[2] M. Oruč, R. Sunulahpašić - "Savremeni metalni materijali" – Univerzitet u Zenici, Fakultet za metalurgiju i meterijale – Zenica, 2005.

[3] Stjepan Kožuh: "Specijalni čelici - skripta", Sveučilište u Zagrebu, Metalurški fakultet, Sisak, 2010.

[4] http://www.worldstainless.org (december 2019)

[5] www.sustainablestainless.org (december 2019)

[6] http://www.isf.de/de/literatur/artikel/paper_733.html (december 2019)

[7] http://rspublication.com/ijst/june12/20.pdf (december 2019)

[8] K. Hribar: ″Vpliv kovinskih in nekovinskih dodatkov na obliko vključkov in tehnološke lastnosti jekel″, Magistrsko delo, Jesenice, 1981

[9] http://www.cartech.com/techarticles.aspx?id=1604 (december 2019)

[10] www.substech.com (december 2019.)

[11] Hillert M. – "Phase equilibria, phase diagrams and phase transformations – The thermodynamic basis", Cambridge university press, 1998

[12] http://www.google.com/patents/US4881990 (december 2019)

[13] Vinograd M. I., Gromora G. P. – " Inclusions in steels and alloys", Publisher "Metallurgy", Moskva, 1972

[14] Babahmetović H. i dr. – "Razvoj i razrada savremenih metalografskih metoda identifikacije sadržaja i vrste nemetalnih uključaka kod kvalitetnih čelika", Metalurški institut "Hasan Brkić", Zenica, 1990

[15] D. Mujagić – "Doprinos istraživanju uticaja mikrolegiranja sa borom, cirkonijem i telurom na osobine austeninog nehrđajućeg čelika sa dodatkom sumpora X8CrNiS18-9", doktorska disertacija, Univerzitet u Zenici, Metalurško – tehnološki fakultet, Zenica, 2017